

Article

Processing of Advanced Battery Materials—Laser Cutting of Pure Lithium Metal Foils

Tobias Jansen ^{*}, David Blass , Sven Hartwig and Klaus Dilger

Institute of Joining and Welding, Technische Universität Braunschweig, Langer Kamp 8, 38106 Braunschweig, Germany; d.blass@tu-braunschweig.de (D.B.); s.hartwig@tu-braunschweig.de (S.H.); k.dilger@tu-braunschweig.de (K.D.)

* Correspondence: tobias.jansen@tu-braunschweig.de; Tel.: +49-531-391-95596

Received: 7 June 2018; Accepted: 20 July 2018; Published: 6 August 2018



Abstract: Due to the increasing demand for high-performance cells for mobile applications, the standards of the performance of active materials and the efficiency of cell production strategies are rising. One promising cell technology to fulfill the increasing requirements for actual and future applications are all solid-state batteries with pure lithium metal on the anode side. The outstanding electrochemical material advantages of lithium, with its high theoretical capacity of 3860 mAh/g and low density of 0.534 g/cm³, can only be taken advantage of in all solid-state batteries, since, in conventional liquid electrochemical systems, the lithium dissolves with each discharging cycle. Apart from the current low stability of all solid-state separators, challenges lie in the general processing, as well as the handling and separation, of lithium metal foils. Unfortunately, lithium metal anodes cannot be separated by conventional die cutting processes in large quantities. Due to its adhesive properties and toughness, mechanical cutting tools require intensive cleaning after each cut. The presented experiments show that remote laser cutting, as a contactless and wear-free method, has the potential to separate anodes in large numbers with high-quality cutting edges.

Keywords: production strategies; cutting; influence of dew point; all solid-state battery production

1. Introduction

The development of future electric mobility is indicated by a highly efficient, conservative and environmentally-friendly technology. Long-term structural changes of energy production systems, from conventional nuclear power and fossil energy sources, such as coal, natural gas and petroleum, to the more ecological production of electricity using renewable energies from hydropower, wind and solar radiation, empower the electric mobility transition tremendously. The key technology to preserve the sustainability of these energies in driving systems are advanced production strategies and materials for high performance mobile electrical storage systems [1].

1.1. State of the Art Lithium Ion Batteries

The continuous development of electric mobility, driven by the automotive industry, is leading to increasing standards for lithium-ion batteries, in terms of safety, cycling stability, specific energy and energy density. Furthermore, the demand for lithium ion batteries is increasing tremendously fast. Conservative estimates indicate a need for almost 160 GWh/a for general storage systems in Europe by 2025. To overtake conventional battery systems in the market by then, three Gigafactories (each 35 GWh/a) have to be built to generate the production capacities [2]. For a feasible, economical and ecological implementation of those production capacities, the conventional electrochemical systems and their production lines must be enhanced and/or new systems and production strategies must be developed.

The established cell system in the automotive sector consists of conventional liquid lithium ion cells, namely, lithium nickel cobalt aluminum oxide (NCA), lithium iron phosphate (LFP) and lithium nickel manganese cobalt oxide (NCM 111) cathodes and graphite anodes. The latter electrochemical system is the special focus of automobilists and is subject to constant development. Future deployed systems are NCM cathodes with an increased nickel content, such as NCM 811 layer oxides and composite graphite anodes doped by silicon to increase the capacities. However, these systems still provide potential for improvement on the cathode and anode side (Figure 1).

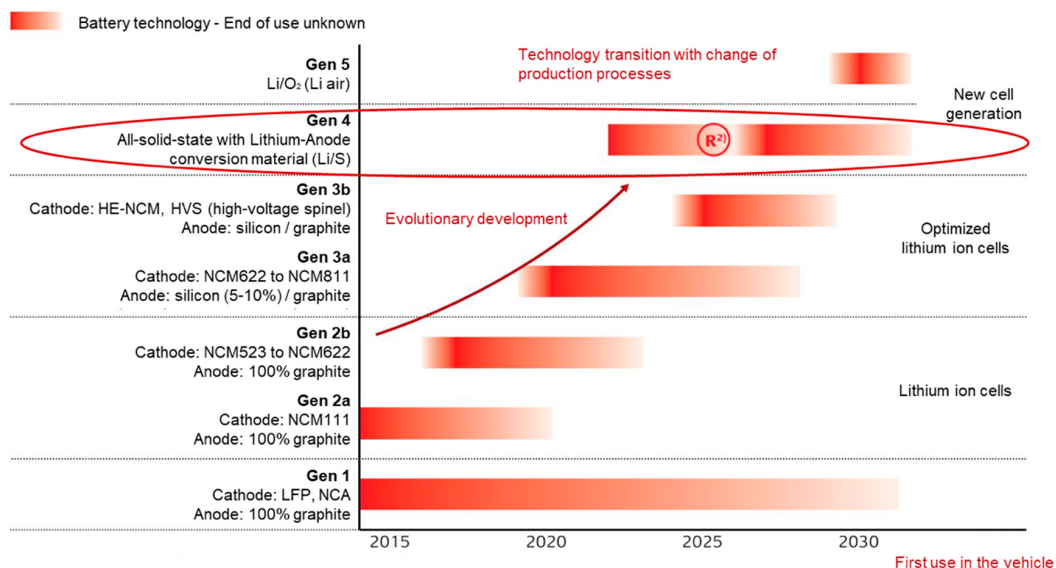


Figure 1. Expected electrochemical technology development for first use in a vehicle; In reference to source: NPE AG2 Batterietechnologie [2].

Promising cell systems compared to the conventional liquid lithium ion cells are all solid-state lithium ion batteries (ASLiBs) with pure lithium metal anodes. Lithium metal anodes are considered to be the most performant anode material for lithium ion electrochemical systems due to their low negative electrochemical potential of -3.040 V compared to a hydrogen electrode.

Furthermore, ASLiBs with those anodes show the potential to reach higher volumetric and gravimetric energy density due to their high theoretical capacity of 3860 mAh/g , and their low density of 0.534 g/cm^3 of pure lithium, which is the lowest density of all solid elements. Thus, very thin and light anodes can be realized, which enable cells with high energy densities. Due to the solid electrolyte, bipolar systems (Figure 2) can be implemented in addition to conventional battery systems. These allow for an increase in the energy density on the battery level [3–5].

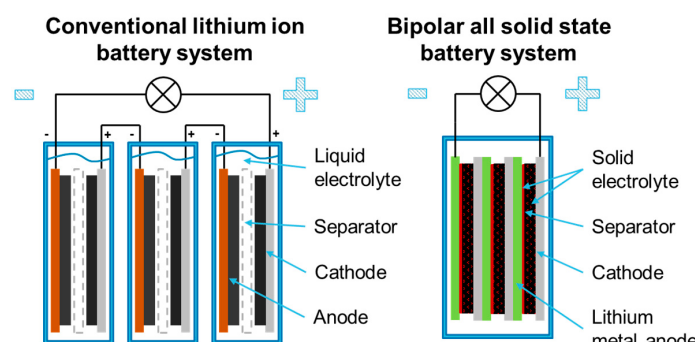


Figure 2. Schematic construction of a conventional and a bipolar lithium ion battery.

Another advantage is that, these cells are safer, as the easily flammable liquid electrolyte is replaced by a solid ceramic or polymer electrolyte (SE), which is not highly flammable. Due to the mechanical and chemical stability of the SE, only a reasonable application of pure lithium metal anodes is possible; as in conventional lithium ion cells with a liquid electrolyte, these kinds of anodes are not stable. The liquid electrolyte leads to an uncontrolled decomposing of the lithium metal anode during the discharge of the cell by dissolving processes. The increased lithium ion concentration in the electrolyte and the inhomogeneity of the anode surface caused by the dissolving processes lead to an uncontrolled plating of the lithium during charging and therefore enhances the dendrite growth. In addition, the lithium reacts with the electrolyte and cannot be recovered during the charging process, making the cell deplete the lithium. In the short and medium term, these dendrites induce micro shortcuts and therefore the death of the cell [3].

Beyond these benefits of the SE, the separator causes problems in exploiting the high capacity of the material, since the interfacial resistance between the SE and the electrodes is very high. This resistance is caused by the creation of an interphase layer with low ionic conductivity, which leads to a loss in performance. Nevertheless, all solid-state lithium ion batteries enable the usability of the promising lithium metal anodes, about which no strategies or processes for mass production are known so far [6].

1.2. State of the Art Cutting of Electrodes

The laser cutting process has become one of the standard solutions in the field of industrial separation application. In addition to cw-lasers, pulsed laser systems are the focus of industrial applications for very accurate cutting edges for sensitive and thin materials. The reason for the use of pulsed laser systems is the high-frequency energy input at a very high power for a very short time (fs-ns). These short pulses keep the heat conduction in the cutting zone very low and thus reduce the occurrence of melt formation at the cutting edge too. Due to the high traversing speed and the associated short cycle time, only the remote laser cutting process is relevant for industrial use or high-throughput production for the separation of electrodes. Due to their mass inertia, mechanically-guided welding optics do not deliver the accuracy and speed of the favored remote optics. In the scientific landscape, the method of remote laser cutting conventional endless Electrode foils (NMC, NCA, LFP cathodes or graphite anodes) is widely discussed [7–10].

However, remote laser cutting is not state of the art in a conventional lithium ion battery production line, even though it is a highly reproducible, wear-free and flexible cutting method. At present, die cutting is the leading process in conventional production lines, since the contamination of metal spatters and active material particles induced by the laser material interaction is not sufficiently investigated. The effects on cell performance and safety are not exactly known and thus the contamination effects on a production line for a mass production cannot be predicted.

Currently, no scientific investigations on the separation of lithium foil or concepts for manufacturing on an industrially relevant scale for ASLiBs with lithium metal anodes have been conducted or published. This is due to the fact that only a small number of lithium anodes are needed on the research level at the moment, and the influence of production strategies for larger quantities has not been the focus of current research. In addition, the commercial application of ASLiBs with lithium anodes is futuristic and therefore no further studies are available for efficient and ecological mass production.

On the laboratory scale, the separation of lithium of a certain shape is done by a simple manual die cutting process or cutting tools (e.g., scissors), which have to be cleaned after each application. This intensive cleaning is necessary because the lithium starts to adhere to the cutting tool after the first interaction. Subsequently, adhering material causes problems in terms of cross contamination, unreproducible cutting edge qualities and therefore unreproducible electrochemical performance. The basic cause for the strong mechanical interlocking of lithium metal on these tools is the significant plastic deformation at low strain. Consequently, for an industrial application, the established die

cutting processes or contacted afflicted processes in general are not suitable for high throughput separation. The adhering of lithium metal on a cutting tool is shown in Figure 3.

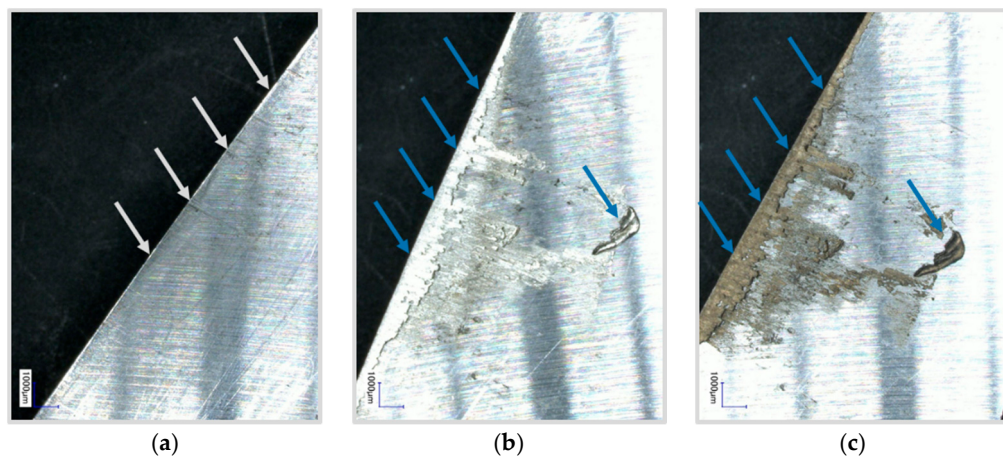


Figure 3. Mechanical cut out. Adhering lithium metal parts are highlighted by the blue arrows. (a) Unused cutting tool; (b) Cutting tool after 5 cuts; (c) Reactions with unconditioned atmosphere.

Another challenge in the processing of lithium is the high reactivity, and therefore the separation and the handling must be performed under certain atmospheric operating conditions. Due to the high reactivity of the lithium with water to lithium hydroxide and hydrogen, cell manufacturing is only possible in a very dry atmosphere. The reaction of the adhering lithium with water in an unconditioned moist atmosphere can be seen in Figure 3c.

All factors shown explain why laser cutting can be regarded as a key technology, which will enable a high automation and throughput speed, since it is a high speed, highly accurate, wear-free and contactless separation method. Nevertheless, this technology also carries risks, as the lithium can be ignited, and a metal fire can be initiated due to the concentrated energy input and the reaction with components of the process atmosphere.

2. Experimental Set-Up

In the presented study, a ns-pulsed fiber laser (1062 nm) with an average power of 72 W and a peak pulse power of up to 13 kW (G4 Pulsed Fiber Laser, SPI Lasers UK Ltd., Southampton, UK) was used. The beam guidance and focusing was performed by a 3-axis laser beam deflection system (AXIALSCAN 30/FOCUSSHIFTER, Raylase AG, Wessling, Germany) with a working field of $400 \times 400 \text{ mm}^2$. The first two dimensions of this remote process allow the cutout of definite geometry whereas the third dimension maintains the focus position on the working field level to ensure a constant spot size of $\sim 90 \mu\text{m}$. The composition of the atmosphere is expected to have a high impact on the cutting edge quality, an effect that was also investigated in this study. Therefore, the cutting experiments were performed under two different conditions with a controlled humidity, once with a dew point of -30°C and once with -15°C . Since the entire plant is housed in a drying room, these dew points could be implemented without any problems. In order to reduce the effects of progressive chemical reactions with the atmosphere, the specimens were analyzed directly after processing and still at dew point of -30°C . Concerning the safety issues, the lithium sheets were cut on a flat sanded steel plate with a groove in the cutting zone to avoid a reaction with the steel plate. The focus of the Laser has been on the same level as the steel plate. The subject of this study was a $50 \mu\text{m}$ thick high-purity lithium foil from Rockwood Lithium. This experimental set-up allows investigations of the influence of the pulse overlap (PO), considering different cutting speeds (V_c), pulse repetition frequencies (PRF) and dew points on the cutting edge quality, as one of the main process quality parameters. In order to ensure a reproducible evaluation of the cutting edges, a light microscope (VHX 2000, Keyence, Osaka, Japan)

and a laser scanning microscope (VK-X Series 3D Laser Scanning Confocal Microscope (LSM), Keyence, Osaka, Japan) were used for the analysis. Melt spatters, melt superelevation and melt formation width are the repetitive features of the generated cut edges. A low melt superelevation as well as a small melt formation width characterize a good cutting edge. The analysis and the mentioned characteristics are shown in Figure 4.

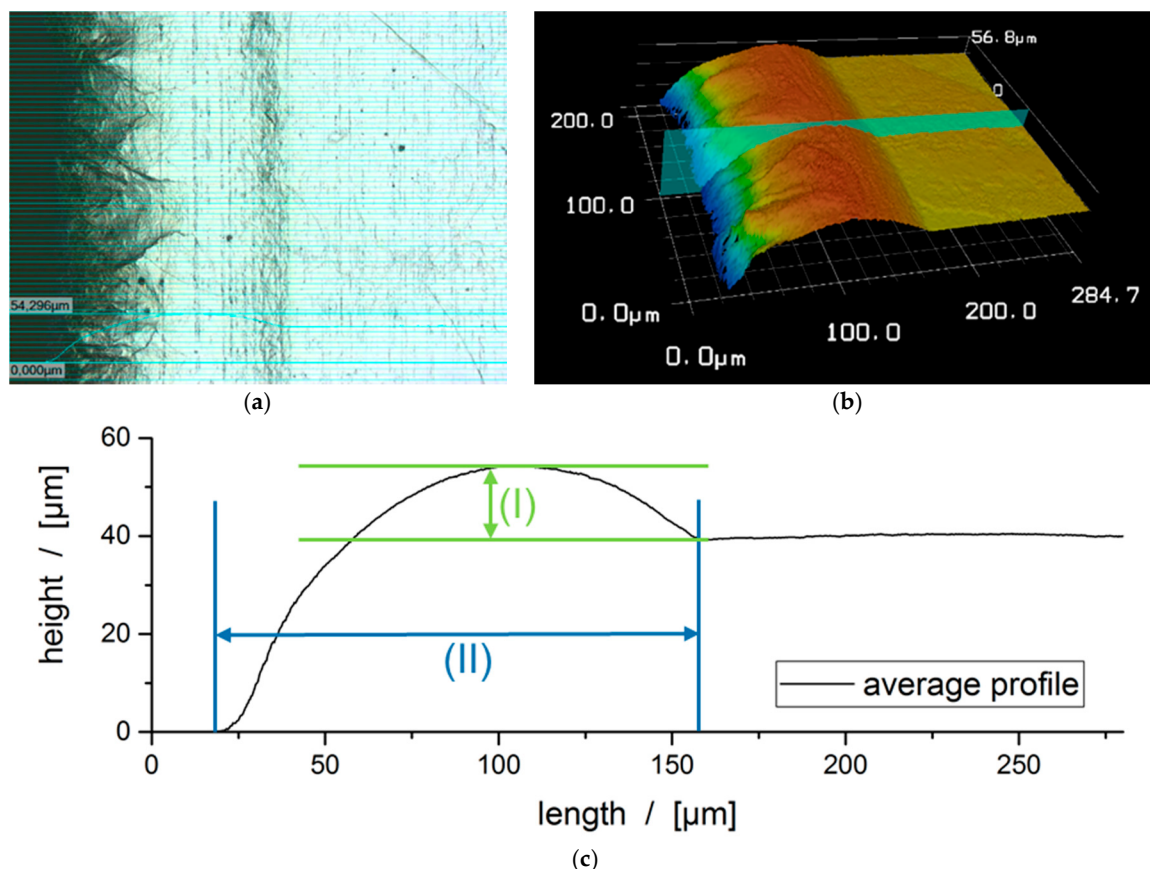


Figure 4. Analysis of a laser cut lithium sheet of 50 μm thickness: (a) Light microscope section; (b) Laser scanning microscope sections; (c) Schematic representation, (I) Melt formation width, (II) Melt superelevation; Laser plant parameters: 350 kHz; 240 ns; 150 mm/s.

Especially, the width of the melt formation is a critical cutting edge feature, since the lithium in this zone has been transferred completely into the molten state. The molten state as well as the high temperatures lead to increasing reactivity of the lithium with water, oxygen and even nitrogen, which is one of the major components of the investigated process atmosphere. In conventional lithium ion cells, the melt superelevation is known to be a critical factor due to the increasing risk of a short circuit, caused by piercing through the separator. For lithium metal anodes, the reason for the risk of superelevation is different, as lithium metal is too soft to pierce the ceramic separator. The different heights can lead to critical peak current densities and thus promote unintended side reactions or the growth of dendrites.

The quality features shown in Figure 4 can essentially be influenced by the pulse repetition frequency and cutting speed. However, previous investigations have shown that for pulsed laser systems these parameters cannot be considered separately. Furthermore, it is necessary to consider the stated parameter pulse overlap. This describes the relationship between the scanning speed of the pulse repetition frequency and the spot size as follows [11]:

$$PO = \left(1 - \frac{v_c}{PRF \cdot d_{spot}} \right) \cdot 100\% \quad (1)$$

The pulse overlap is defined by the pulse repetition frequency, the cutting speed and the spot size d_{spot} . Since the spot size is constant, high PRF and low V_c lead to high PO . The investigations carried out in this experiment are intended to show how the cutting edge quality depends on the V_c and the PO . Therefore, a test matrix was created in which the PRF was varied from 70 to 490 kHz and combined with a V_c variation from 50 to 150 mm/s.

The evaluation of the chemical contamination caused by the varied water concentration in the process atmosphere was performed by an SEM (FEI Quanta 650, Thermo Fisher, Waltham, MA, USA) and an EDX (Oxford X-Max 80 mm², Oxford instruments, Abingdon, England). The atmosphere was kept constant until the already-mentioned analyses were performed in a vacuum, so that no significant contamination could occur.

Shortly after the laser material interaction at a dew point of -30°C , no contamination could be detected and thus a methodology was developed to amplify and evaluate the effects. In order to be able to adequately evaluate the atmospheric effects during the cutting process, the cutting samples were stored for 5 months at a dew point of -60°C . The aging causes an ongoing reaction of the lithium with the remaining components of the atmosphere, which enables the evaluation of the chemical stability of the cutting edge depending on the process parameters and geometric shape.

3. Results

The results of the investigation of the influence of the pulse overlap and the process atmosphere on the physical and chemical properties of the cutting edge are considered separately. At first, the results of the influence of the laser and system parameters on the physical cutting edge properties at a constant dew point of -30°C are presented. For this purpose, the influence of the cutting speed on the cutting edge quality is analyzed on the basis of light microscope and laser scanning microscope images. In the following, the interaction between the cutting speed and the pulse repetition frequency in the form of the pulse overlap and its influence on the geometric properties of the cut edge are shown.

In addition to the images mentioned above, SEM and EDX images are analyzed for further investigations to evaluate the influence of the dew point on the laser material interaction. With the help of a superimposition of the images, the chemical properties of the cutting edge can be assessed in addition to its physical properties. Finally, material defects, which lead to detrimental effects and significantly affect the quality and safety of the cutting process, will be discussed.

3.1. Influence of the Cutting Speed at A Dew Point of -30°C

The investigations to determine the influence of the cutting speed is the main focus of this process technology evaluation. For this purpose, lithium foil was cut with a constant power, pulse repetition frequency, pulse duration and dew point along with variable cutting speeds. The result of the fastest three cutting speeds is illustrated by the light microscope images in Figure 5.

The light microscope images clearly show that the cutting speed can greatly influence the melt formation width at the cutting edge. The analysis of the images shows a reciprocal dependence of the melt formation width on the cutting speed. The faster the cut, the smaller the width of the melt formation. Using a linear fit, this decrease can be estimated in the examined process window by a ratio of melt formation width to cutting speed of -2.75 ($\mu\text{m s}$)/mm with an R-square of 0.97 at a pulse repetition frequency of 490 kHz. The cutting experiments at 350 kHz result in a slightly higher value of -3.06 ($\mu\text{m s}$)/mm. Due to the higher standard deviation at 350 kHz, an R-square of 0.732 is derived.

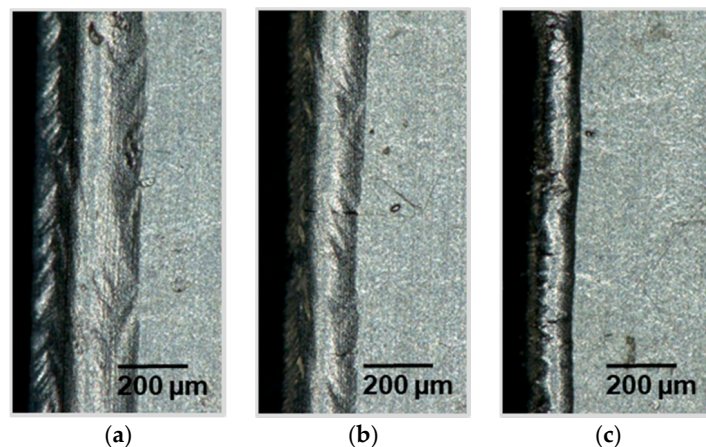


Figure 5. Light microscope sections of a laser cut lithium sheet: 72.8 W, 490 kHz, 240 ns; (a) 75 mm/s, PO 99.83%; (b) 100 mm/s, PO 99.77%; (c) 150 mm/s, PO 99.66%.

The resulting melt formation widths for the four investigated cutting speeds are shown in Figure 6. Pulse repetition frequencies of 350 and 490 kHz result in a quasi-linear trend, wherein the standard deviation at 490 kHz is slightly lower. It can also be seen that smaller melt formation widths can be achieved at lower cutting speeds with a higher pulse repetition frequency.

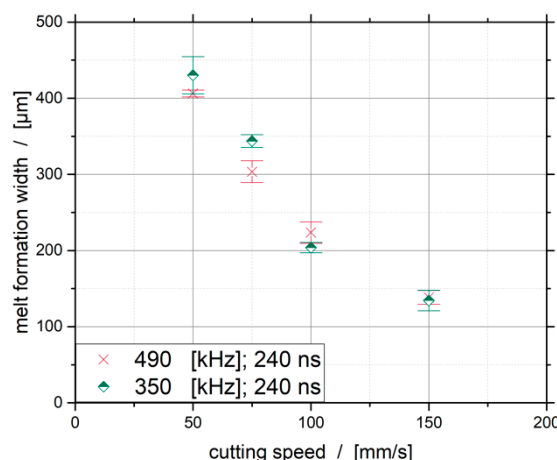


Figure 6. Influence of the cutting speed on the melt formation width.

The influence of the cutting speed on the second evaluation criterion of the cutting edge, the melt superelevation, is carried out by the evaluation of topographic images. For this evaluation, the laser scanning microscope images shown in Figure 7 are used to characterize the influence of the investigated cutting speeds at the PRF of 490 kHz.

The LSM-sections in Figure 7 clearly show that the cutting speed significantly influences the melt superelevation. The increase in melt superelevation grows steadily with the increasing cutting speed. Furthermore, it can be seen that the shape of the melt superelevation is subject to change. The descriptive radius of the melting form decreases steadily with the increasing cutting speed. At the highest speed of 150 mm/s, in addition to the homogeneous formation of the molten bath, local extreme elevations can be detected, which can reach a value of up to 37 μm . The average evaluation of the melt superelevation, as explained in the experimental setup, takes into account the artifacts that occur on the resulting melt pool only to a small extent, as shown in Figure 7c.

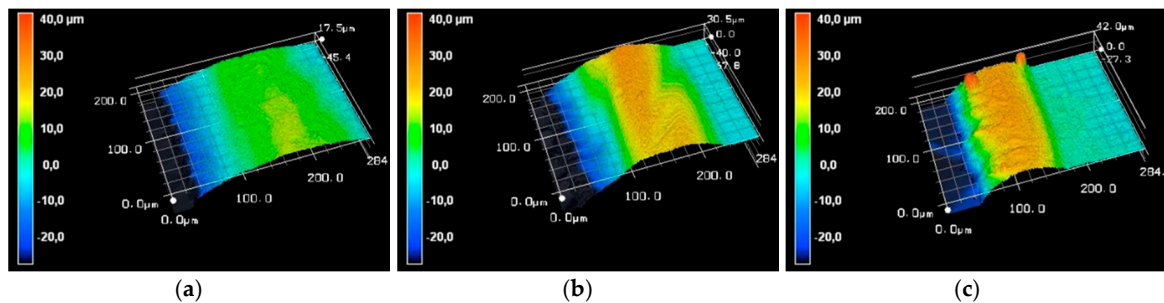


Figure 7. Laser scanning microscope sections of a laser cut lithium sheet: 72.8 W, 490 kHz, 240 ns; (a) 75 mm/s, PO 99.83%; (b) 100 mm/s, PO 99.77%; (c) 150 mm/s, PO 99.66%.

The influence of the cutting speed on the melt superelevation, for the frequencies of 350 and 490 kHz at a dew point of -30°C , is shown in Figure 8. The evaluation of these results shows that the lowest melt superelevation can be achieved at the lowest speed. At the lowest as well as at the highest investigated cutting speed, the lower pulse repetition frequency leads to a lower melt superelevation. The results show that there is a clear dependency between the melt superelevation and the cutting speed for both investigated frequencies.

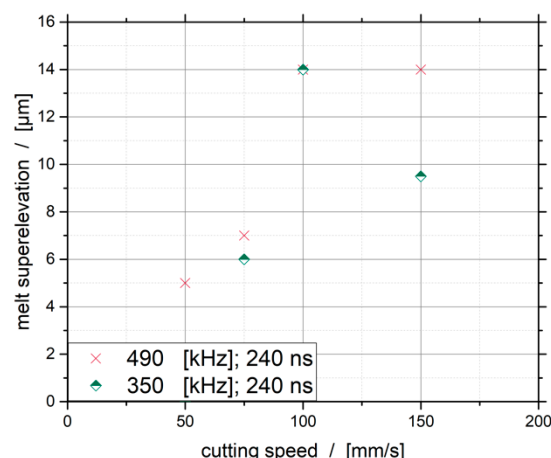


Figure 8. Influence of the cutting speed on the melt superelevation.

3.2. Influence of the Pulse Overlap at a Dew Point of -30°C

When cutting with a pulsed laser system, the laser-material interactions can only be represented accurately by the parameter pulse overlap. This correlates with traversing speed and the pulse repetition frequency, and it describes the continuity of the energy input in the separation zone. The influence of pulse overlap on the homogeneity of the molten bath is shown in Figure 9. The different pulse overlaps were generated by a variation of the cutting speed, while the pulse repetition frequency and the spot diameter were kept constant.

The light microscope images in Figure 9 show that from a pulse overlap below roughly 99.44% (c) it is no longer possible to form a homogeneous molten bath. An undershot of this value leads to an uncontrolled formation of metal spatters and to an inhomogeneous distribution of the melting width and melt superelevation. These metal spatters can reach maximum elevations of up to 48 μm and are therefore well above the average elevation of 14 μm with a pulse overlap of 99.58% (b).

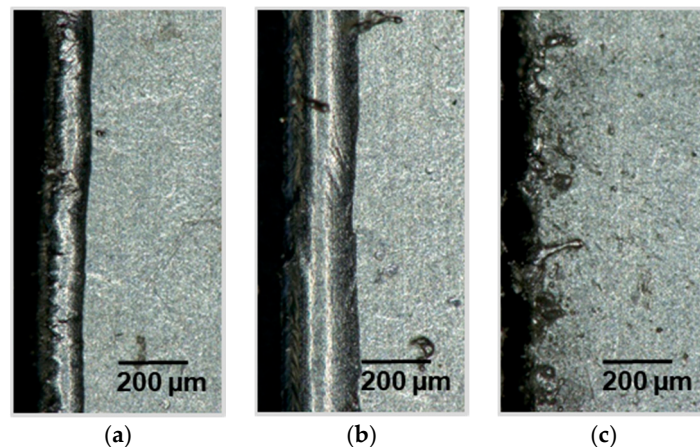


Figure 9. Light microscope sections of a laser cut lithium sheet: 72.8 W, 200 kHz, 240 ns; (a) 50 mm/s, PO 99.72%; (b) 75 mm/s, PO 99.58%; (c) 100 mm/s, PO 99.44%.

A dependence of the formation of a homogeneous molten bath on the pulse overlap can already be confirmed by this series of experiments. However, to get a deeper understanding, additional experiments were performed to determine whether these findings can be attributed to the pulse overlap or can only be explained by the varied cutting speed and relevant energy input. For this purpose, sections with varying pulse overlaps were generated by a variation of the pulse repetition frequency at a constant cutting speed and spot size.

Selected light microscope images of these cutting experiments, for a cutting speed of 100 mm/s, are shown in Figure 10. The cutting edges (a) and (b) of Figure 10 show that no homogenous molten bath can be formed at the low pulse repetition frequencies. These cutting edges are characterized by large variations in melt formation width and melt superelevation. In addition to the uncontrolled formation of metal spatters on the surface of the electrode, the cutting edge profile is characterized by severe unevenness or roughness. A frequency of 350 kHz results in a pulse overlap of 99.68%, (c) which is sufficient for the formation of a homogeneous molten bath. This series of experiments complements the findings from previous investigations, which indicate that the PO is the essential setting parameter for the generation of a homogeneous molten bath. Beyond these findings, a further analysis of the data shows that the pulse overlap affects the width of the melt formation. For this purpose, the results of the investigated frequencies (200, 350, 490 kHz) and cutting speeds (50, 75, 100, 150 mm/s) in the form of the pulse overlap were plotted against the melt pool width.

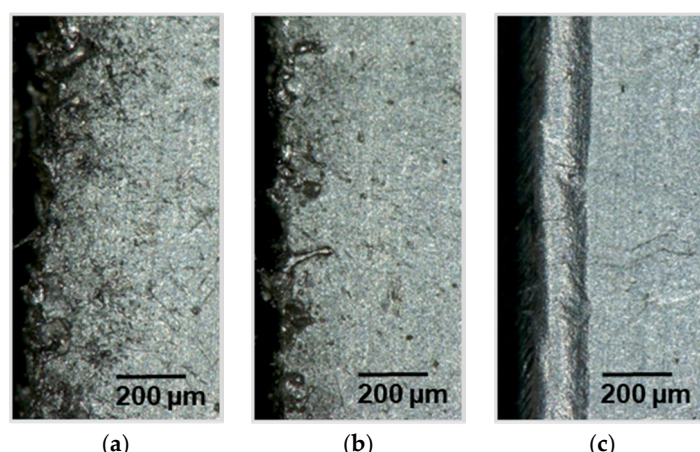


Figure 10. Light microscope sections of a laser cut lithium sheet: 72.8 W, 100 mm/s, 240 ns; (a) 70 kHz, PO 98.41%; (b) 200 kHz, PO 99.44%; (c) 350 kHz, PO 99.68%.

The investigated frequency of 70 kHz was no longer taken into account because it leads to an uncontrolled formation of molten metal at all investigated cutting speeds. The generated diagram is shown in Figure 11. In addition to these data, the diagram shows the minimum necessary pulse overlap to produce a homogeneous melt pool of 99.58%.

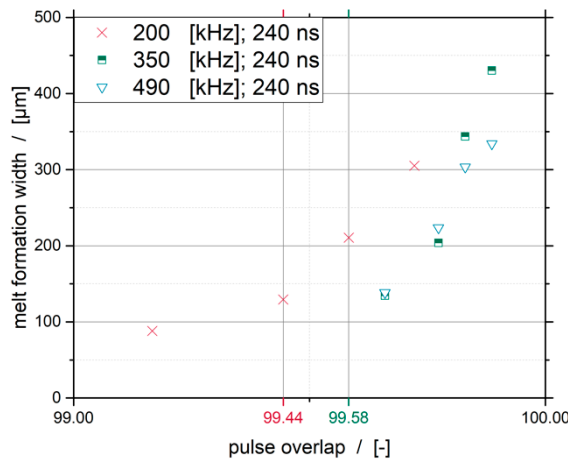


Figure 11. Influence of the pulse overlap on the melt formation width for a pulse width of 240 ns.

With a pulse overlap below 99.44%, it is no longer possible to produce a homogeneous molten bath. Beyond these statements, it can be seen that, with a decreasing pulse overlap, the melt formation width decreases until the said zone is reached. Furthermore, it is shown that higher pulse repetition frequencies lead to a smaller formation of the melting width with similar pulse overlaps.

In order to investigate the influence of the pulse length, cuts were performed with the same pulse overlap and energy input, but with shortened pulse lengths (Figure 12). The results show that with shorter pulses no homogeneous melt pool can be produced. Higher pulse overlaps with short pulses do not lead to a molten bath at all. However, the cutting edges are characterized by very high melt superelevation peaks.

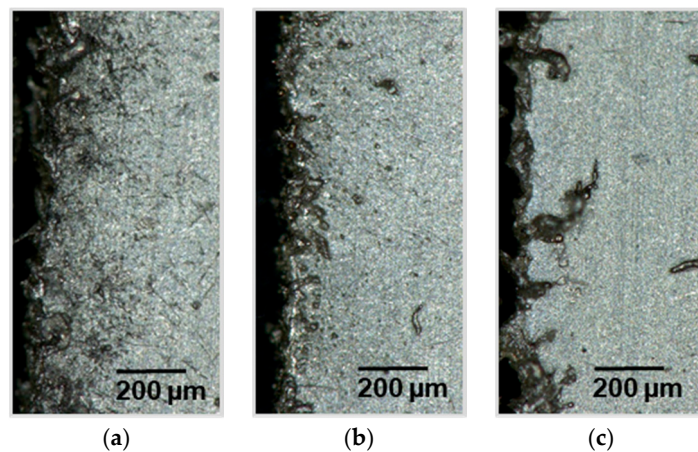


Figure 12. Light microscope sections of a laser cut lithium sheet: 72.8 W, 100 mm/s; (a) 70 kHz, 240 ns, PO 98.41%; (b) 200 kHz, 55 ns, PO 99.44%; (c) 350 kHz, 26 ns, PO 99.68%.

3.3. Influence of Atmospheric Conditions in Terms of Different Dew Points

In addition to the laser and system parameters, the humidity of the process atmosphere in particular has a strong influence on the processability of the lithium foil and on the quality of the cutting edge. To evaluate this influence, additional cutting tests were carried out at a dew point of

-15°C to complement those at the -30°C dew point. Cutting edges that were processed at different pulse overlaps, and the relevant cutting speeds at a dew point of -15°C , are shown in Figure 12.

The light microscope images in Figure 13 show that, at a dew point of -15°C , the lithium reacts intensively with the water contained in the process atmosphere during the cutting process. It can be observed that a blackish discolored deposition is formed. At the cutting speeds of 50 mm/s (a) and 100 mm/s (b), these deposits are not located directly at the cutting edge, but rather start at a distance of 50 μm from the cutting edge. At the highest tested velocity of 150 mm/s (c), the deposits begin directly at the cutting edge. Furthermore, the cutting series shows that with an increasing cutting speed or with a decreasing energy input, this discoloration steadily decreases.

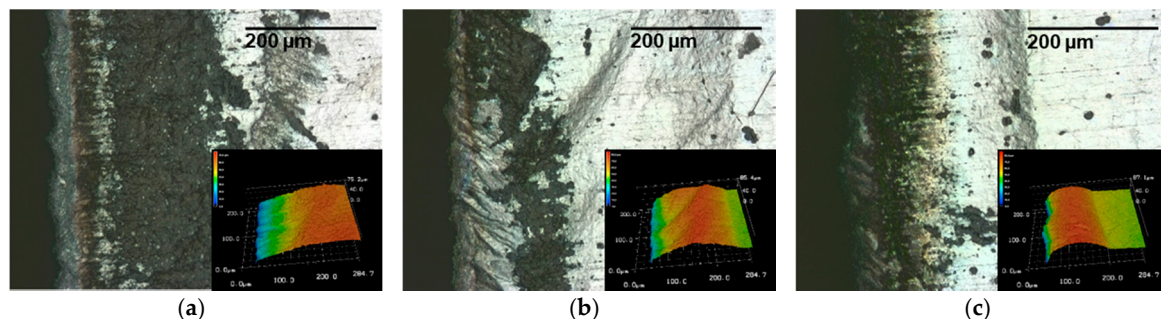


Figure 13. Light and laser scanning microscope sections of a laser cut lithium sheet: 72.8 W, 490 kHz, 240 ns, dew point -15°C ; (a) 50 mm/s, PO 99.89%; (b) 100 mm/s, PO 99.77%; (c) 150 mm/s, PO 99.66%.

With the same laser and system parameters, at a lower dew point of -30°C , these black deposits cannot be identified by light microscope images (Figure 14). An influence of the laser system parameters on the degree of contamination therefore cannot initially be determined.

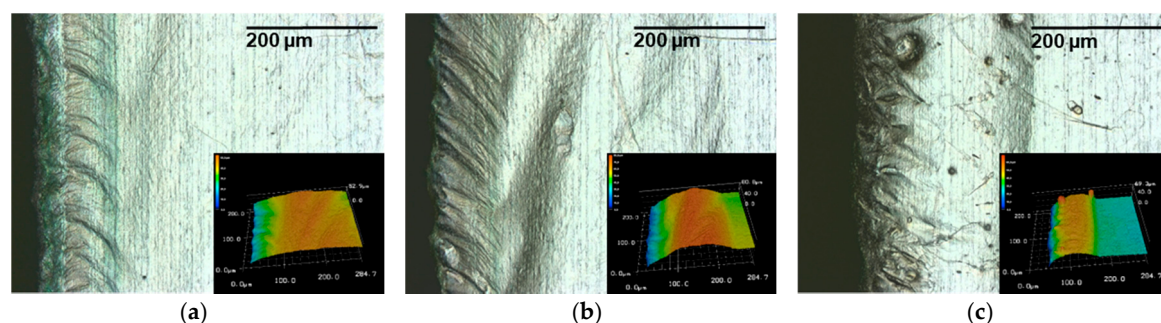


Figure 14. Light and laser scanning microscope sections of a laser cut lithium sheet: 72.8 W, 490 kHz, 240 ns, dew point -30°C ; (a) 50 mm/s, PO 99.89%; (b) 100 mm/s, PO 99.77%; (c) 150 mm/s, PO 99.66%.

The evaluation of the melting width for the examined dew points shows that with the same cutting parameters, the physical characteristics of the cutting edge are less pronounced at lower dew points.

This issue is illustrated by the diagram in Figure 15. At speeds of 50 mm/s and 75 mm/s, the melting width at the lower dew point is about 100 μm smaller. With a speed of 100 mm/s, the influence decreases and the differences are in their standard deviations. Furthermore, it can be seen that, at high speeds, the melting width and the standard deviation for the dew points investigated are approximately 130 μm .

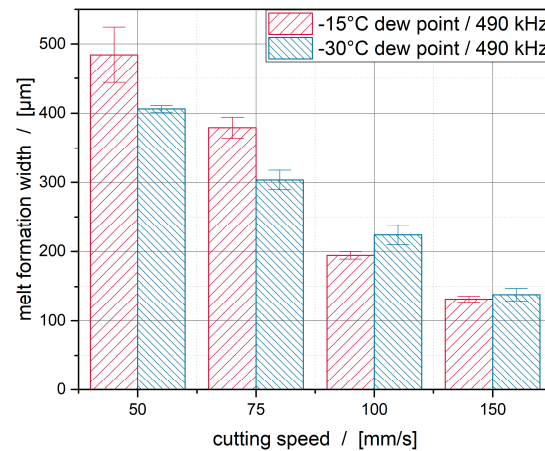


Figure 15. Influence of the cutting speed and dew point on the melt formation width.

The preceding process investigations show that a dew point of $-30\text{ }^{\circ}\text{C}$ is sufficient to separate the lithium foil, which is apparently contamination-free. Since no contamination or reaction products, at a dew point of $-30\text{ }^{\circ}\text{C}$, can be seen by the light microscope images, these cutting edges were subjected to controlled aging. For this, the samples were aged at a constant dew point of $-60\text{ }^{\circ}\text{C}$ for 5 months. Due to the slow reaction of lithium with the remaining water in the atmosphere and with nitrogen, the precursor initiated by the laser material interaction in the separation zone becomes larger and thus identifiable by progressive reaction. This allows an evaluation of the process material interaction for the investigated laser and plant parameters at a dew point of $-30\text{ }^{\circ}\text{C}$. Two results of these investigations are shown in Figure 16.

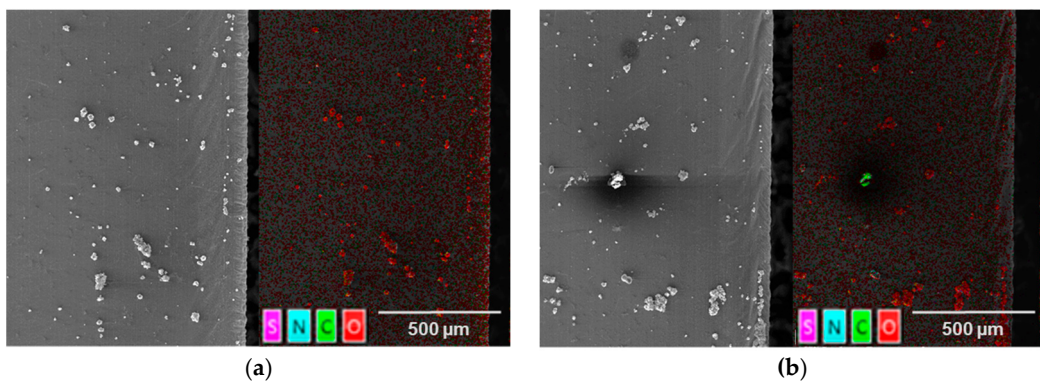


Figure 16. SEM (left) and EDX (right) section of a laser cut lithium sheet: 72.8 W, 490 kHz, 240 ns, dew point $-30\text{ }^{\circ}\text{C}$; (a) 50 mm/s; PO 99.89%; (b) 100 mm/s; PO 99.77%; after 5 months of aging in an atmosphere with a dew point of $-60\text{ }^{\circ}\text{C}$.

The images in Figures 16a,b and 17 are divided into two parts. On the left side, the SEM image is shown and, on the right side, the same SEM image, superimposed with the results of the EDX measurement, is shown. The superimposed SEM/EDX images (Figure 16a,b, right) show that only a small amount of reaction products, caused by the laser material interaction, occur in the area of the cut edge. For both the cutting speeds of 50 mm/s and 100 mm/s, only very few oxides can be identified in the area of the separation zone. The reaction products occurring within this region are also not directly at the cutting edge, as observed in the experiments at a dew point of $-15\text{ }^{\circ}\text{C}$. The deposition of the reaction products begins at about 50 microns away from the cutting edge. This area is characterized by the start of the superelevation of the melting. Oxides can also be identified further away from the cutting edge. A clear origin of these reaction products cannot be made on the basis of these analyses.

Aging of the highest investigated cutting speed of 150 mm/s, at a dew point of -30°C of the process atmosphere, leads to the cutting edge shown in Figure 17.

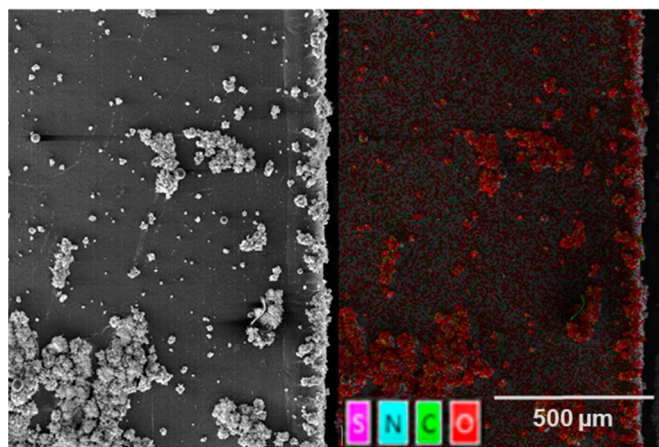


Figure 17. SEM (left) and EDX (right) section of a laser cut lithium sheet: 72.8 W, 490 kHz, 240 ns, dew point -30°C , 150 mm/s; PO 99.66%; after 5 months of aging in an atmosphere with a dew point of -60°C .

Using the EDX analysis, a strong oxide formation can be detected on the SEM image in the area of the cutting edge. In contrast to the results from previous investigations, the oxides can be detected directly at the cutting edge. Furthermore, the abundance and size of these oxides greatly exceed the results from the cutting experiments at lower cutting speeds. In addition to the oxides on the cutting edge, even larger oxide areas on the electrode surface can be identified.

The appearance of these oxides is also characterized by a porous amorphous structure, as in the lower cutting speeds experiments. The shape of these oxides does not follow a uniform structure, but is rather characterized by a diverse shape in width and length. Furthermore, it can be seen that these oxides lie on the surface of the lithium. Due to the undefined structure and the previous evaluations of the light microscope images, these oxides cannot be identified as molten splashes.

3.4. Effects of Defects

With regard to the evaluation of the safety of the laser cutting process, cutting tests were carried out on lithium foils, which have already strongly reacted. The result of these cutting tests is shown in the picture in Figure 18. Despite the low dew point of -30°C of the process atmosphere, the laser material interaction initiated a metal fire of lithium, even though the same cutting parameters were used as in the previously mentioned, uncritical experiments.



Figure 18. Image of lithium metal fire initiated by Laser lithium hydroxide interaction (blue circle); Lithium metal after 1.5 years at a dew point of -30°C ; 72.8 W, 490 kHz, 240 ns, dew point -30°C ; 50 mm/s, PO 99.89%.

The metal fire was initiated at the end of the cutting process. Here, the laser cut ended in a region covered by lithium hydroxide and lithium oxide contaminants. A comparatively large part of this contamination is indicated in Figure 18 by a blue circle. As the laser shut off, the lithium starts to burn. The reaction of the lithium with the oxygen of the process atmosphere led to the formation of lithium oxide, which settles in the form of a white powder on the surface of the cutting device. The metal fire was extinguished by suffocation using a steel plate. Without this intervention, the entire sample would have burned. Due to the low water content in the atmosphere, the reaction rate was moderate.

4. Discussion

Investigations on the influence of the cutting speed on the characteristics of the cutting edge during the laser cutting of lithium metal foils at a dew point of -30°C show that the melting width decreases with the increasing cutting speed. This can be explained by the fact that, at low cutting speeds, the energy input is much higher than at high cutting speeds. Due to the greater energy input, the heat conduction increases and thus a wider area is subject to melt. This increase in the melt formation width also causes the melt superelevation to decrease, as the molten lithium can spread over a larger area. Thus, faster cutting speeds lead to a lower melt formation width, but also a higher melt superelevation occurs.

The increasing width of the melt formation with the increasing pulse overlap supplement the findings from studies on the influence of the cutting speed. In this case, higher pulse repetition frequencies, with a constant pulse length and the same energy input (J/mm), lead to a wider melting area. This is due to the fact that the higher frequency increases the effective laser material interaction time. Due to the longer interaction time, the heat conduction increases, and more material is transferred to the molten state.

To create a homogeneous molten bath, the continuity of the energy input and thus the pulse overlap plays a major role. If the pulse overlap is less than 99.58% (with a pulse length of 240 ns), the distance between pulses is too long to create a stable molten bath by heat accumulation. A dependence of the melt superelevation of the pulse overlap in a homogeneous molten bath cannot be observed.

The realization that a certain pulse overlap is necessary to produce a homogeneous molten bath is to be considered dependent on the pulse length. Shorter pulses at constant frequencies lead to a lower laser-material interaction time and therefore to a lower heat conduction. As a result, less energy can be accumulated in the cutting edge so that no continuous molten bath is formed. With a constant average power and pulse duration, the pulse peak power decreases with the increasing *PRF*. If the pulse duration is shortened to a constant average power, the pulse peak power can be kept constant at a higher *PRF*. Therefore, the experiments with a constant average power and high *PRF* show that cuts with shorter pulse lengths and the relevant high pulse peak powers tend to result in a sublimation cut, whereas longer pulses and the relevant low pulse peak powers lead to fusion cutting. The latter process is due to the very highly achievable homogeneity with the laser system, which is favorably used. The laser material interaction can be characterized by the ratio of the time in which the laser is on and the time in which the laser is off (relative time of interaction). To create a homogeneous molten bath, the continuity of the energy input and thus the relative time of interaction (RTI) has to reach a certain value. If the value is less than 8.4%, the time of interaction is too short to create a stable molten bath at the cutting edge. Lower RTIs have a negative impact on the yield of a homogeneous molten bath. With the same pulse overlap, lower RTIs do not lead to homogeneous molten bath formation.

The water content of the process atmosphere has a significant influence on the contamination of the cutting zone. At a dew point of -30°C no contamination could be identified by light microscopy shortly after cutting. Due to the lower water content, no reaction takes place by reason of the laser-induced energy input. Because of the plasma formation during the cutting process, the separation area is completely insulated from the process atmosphere. As soon as the plasma shifts due to the feed, a homogeneous oxide layer forms. At higher water concentrations, it can be assumed that just

behind the laser-induced plasma, the remaining energy in the lithium melt is sufficient to initiate a reaction with the water. In addition, it should be noted that, at a lower dew point, a wide molten pool is established. This is due to the fact that the hydrogen formation, due to reactions of the lithium with the water contained in the process atmosphere, leads to an additional energy input.

A major influence on the safety of the process is the evaluation of the effects of material defects. The illustrated inflammation of the material has been caused by a material defect. During the cutting process, an area which was characterized by severe contamination of lithium hydroxide and lithium oxide was cut through. Since the material only ignited after the laser had gone out, it can be assumed that the laser plasma was not sufficient to cover the separation zone and thus to prevent the reaction with oxygen. Another cause of the inflammation is the high diffusibility of oxygen by the amorphous lithium hydroxide and lithium oxide layer. Furthermore, the bound oxygen in the named components is a potential source of exothermic reaction.

The aging tests confirm the assumptions made regarding the laser-induced plasma, since lithium oxides form only at a defined distance from the cutting edge. No oxide contamination forms directly on the cutting edge itself, since the plasma has a longer residence time there. Only at higher speeds, the formation of said contamination products extends to the cutting edge.

5. Conclusions and Outlook

The results of this study (Figure 19) show that, at a dew point of -30°C , lithium metal anodes can be safely separated by means of a pulsed laser system. Due to the contactless process and the highly reproducible cutting edge quality, this process can be used for intensive mass production.

The findings show that, for a good molten bath formation, a high pulse overlap is needed. In order to generate faster industrially relevant cutting speeds, investigations should be carried out with higher pulse repetition frequencies and cw laser beam sources. Furthermore, the results show that with a decreasing pulse length, the melt-cutting process goes into a sublimation cutting process. Investigations should be carried out with pulse lengths in the pico second range, since, at the shortest pulse lengths investigated, melt is still formed, which leads to high local melt peaks. These pulse lengths could contribute to the fact that the cutting process is characterized exclusively by sublimation processes and therefore leads to a sharp cutting edge without melt peaks.

Furthermore, further attempts must be made to increase the safety of the process and to reduce the contamination by the process atmosphere.

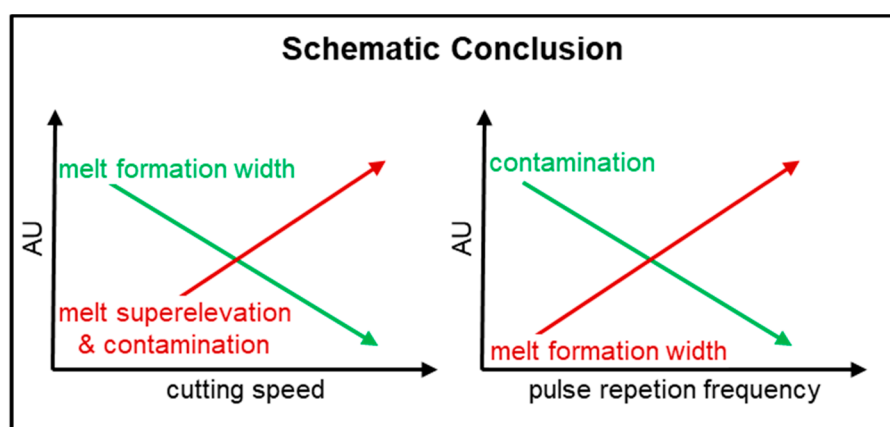


Figure 19. Graphical conclusion of the results (72.8 W, 70–490 kHz, 50–150 mm/s, 240 ns, dew point -30°C).

Author Contributions: T.J. and D.B. wrote and edited the main parts of the paper, S.H. designed the aging experiments and analyzed the REM/EDX data. K.D. administered the research project. All authors contributed to scientific discussions.

Funding: This Paper was not funded by a public project.

Acknowledgments: Hereby I would like to thank my student assistants Hannes Rumpel and Julien Essers for their technical support.

Conflicts of Interest: The authors declare no conflict of interest.

References

1. *Handbuch Lithium-Ionen-Batterien*; Springer: Berlin/Heidelberg, Germany; New York, NY, USA, 2013.
2. Elektromobilität, N.P. *Roadmap Integrierte Zell- und Batterieproduktion Deutschland*; Gemeinsame Geschäftsstelle Elektromobilität der Bundesregierung (GGEMO): Berlin, Germany, 2016.
3. Qian, J.; Henderson, W.A.; Xu, W.; Bhattacharya, P.; Engelhard, M.; Borodin, O.; Zhang, J.-G. High rate and stable cycling of lithium metal anode. *Nat. Commun.* **2015**, *6*, 6362. [[CrossRef](#)] [[PubMed](#)]
4. Zhu, Y.; He, X.; Mo, Y. First principles study on electrochemical and chemical stability of solid electrolyte–electrode interfaces in all-solid-state Li-ion batteries. *J. Mater. Chem. A* **2016**, *4*, 3253–3266. [[CrossRef](#)]
5. Gambe, Y.; Sun, Y.; Honma, I. Development of bipolar all-solid-state lithium battery based on quasi-solid-state electrolyte containing tetraglyme-LiTFSI equimolar complex. *Sci. Rep.* **2015**, *5*, 8869. [[CrossRef](#)] [[PubMed](#)]
6. Wu, B.; Wang, S.; Evans IV, W.J.; Deng, D.Z.; Yang, J.; Xiao, J. Interfacial behaviours between lithium ion conductors and electrode materials in various battery systems. *J. Mater. Chem. A* **2016**, *4*, 15266–15280. [[CrossRef](#)]
7. Lee, D.; Patwa, R.; Herfurth, H.; Mazumder, J. High speed remote laser cutting of electrodes for lithium-ion batteries: Anode. *J. Power Sources* **2013**, *240*, 368–380. [[CrossRef](#)]
8. Luetke, M.; Franke, V.; Techel, A.; Himmer, T.; Klotzbach, U.; Wetzig, A.; Beyer, E. A Comparative Study on Cutting Electrodes for Batteries with Lasers. *Phys. Procedia* **2011**, *12*, 286–291. [[CrossRef](#)]
9. Reincke, T.; Kreling, S.; Dilger, K. The influences of pulse overlap on cut quality during fiber laser cutting of electrodes for Lithium-ion batteries. In Proceedings of the Lasers in Manufacturing Conference, Berlin, Germany, 22–25 June 2015.
10. Dahotre, N.B.; Harimkar, S.P. *Laser Fabrication and Machining of Materials*; Springer: New York, NY, USA, 2008.
11. Kreling, S. Laserstrahlung mit Unterschiedlicher Wellenlänge zur Klebvorberarbeitung von CFK. Ph.D. Thesis, Technische Universität Braunschweig, Braunschweig, Germany, 2015.



© 2018 by the authors. Licensee MDPI, Basel, Switzerland. This article is an open access article distributed under the terms and conditions of the Creative Commons Attribution (CC BY) license (<http://creativecommons.org/licenses/by/4.0/>).